

Response to the comments/ questions from Referee (2)_17 Sept 2014

- (1) Comment: the authors need to be more clear and more precise about the data treatment and model calibration procedures.

We agree with the reviewer and for this we have much extended the two chapters dealing with data treatment and calibration-validation, including sources of inaccuracies. The additions are highlighted in yellow.

- (2) Comment: discussing model discrepancies, where and why they arise?

Model discrepancies have been extensively treated in the new version of the paper. In particular we have explained why the model has failed simulating the sand transport and deposition in the reservoir. The negative effects on the results of applying some modeling techniques such as the morphological factor have been discussed as well.

- (3) Question: can you give indications about the filtering and treatment process and the reasons for this? How where survey performed and what are the associated uncertainties?

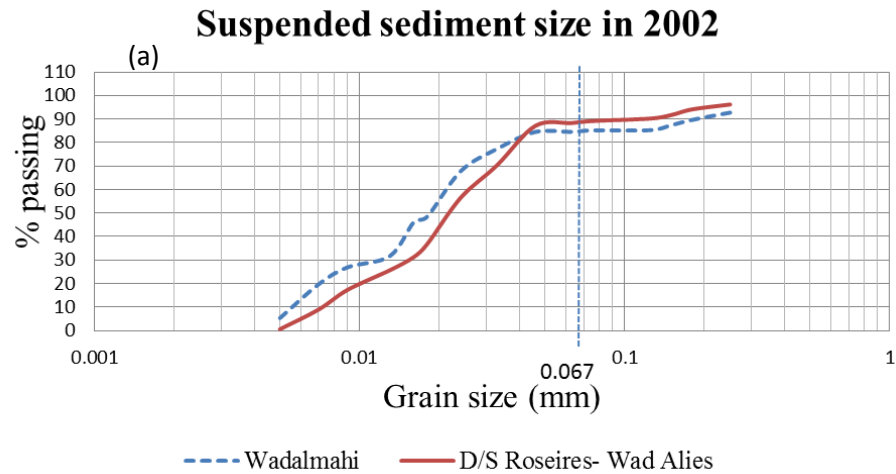
The data were collected from different sources with important differences, for instance in the reference datum. A comparison between the data was executed and inaccuracies and discrepancies were adjusted also with the help of the model. Furthermore, suspended solids data were analyzed to see if the trends of sediment concentration with time compares to the flow magnitude. The new version of the paper has been extended also in the part dealing with the treatment of data.

- (4) Comment: Table1: given the way volumes are estimated an assessment of uncertainty is needed

These values are calculated using the QUICKIN tool available in Delft3D software. The tool computes the volume above the topography up to any certain level. Volumes are calculated for computational grid cells within the domain. The volumes are computed for those cells with four valid depth values (data at cell vertices), it is defined as the mean value of the four surrounding depth values (Delft3D manual, 2010). However, due to the large grid size and the quite large interval between the survey cross sections (2-5 km), the volumes suffer for a high degree of uncertainty, but given the absence of more reliable data it was not possible to estimate the level of this uncertainty.

- (5) Question: how is the sand proportion estimated? What is the bed grain size distribution before the dam?

The sand proportion was estimated based on the grain size distribution of the suspended sediment samples. Normally, suspended sediment (S.S) measurements in Roseires Reservoir are executed during the flood season only. The figure below shows the only available S.S particle size distribution measured in 2002.



In 2002, suspended sediment samples were taken in Wad Almahi station (inside the reservoir) and Wad Alies (downstream of the dam). The figure shows that silt is the dominant type of sediment in suspension, since it represents more than 80% of the sample. Furthermore, sand represents about 15% of the suspended sediment in the reservoir and 10% of the suspended sediment downstream of the dam. We have added and discussed this figure also in the new version of the paper, where it becomes Figure 4.

There is no information available for the grain size distribution before the dam was completed in 1966.

(6) Comment: 5.1 model description

- a. You must provide in a table, and discuss in the text, the values of parameters used (concerning the 3-D effects you mention) and closure coefficients for the k-e model.

#	Physical parameter	The value used	Remark
1	Spiral flow $-(\beta)$	0.5	For $\beta = 0$, the depth- averaged flow is not influenced by the secondary flow.
2	Horizontal eddy viscosity	1.0 (m ² /s)	
3	Horizontal eddy diffusivity	10 (m ² /s)	

The table above is a part of a new table added to the paper. The new table (2) includes the closure coefficients of the k-e model (above) and other calibration parameters. The new version of the paper includes also a better description of how the effects of the spiral flow (a clear 3D flow feature) are parameterized in the 2D model. The new text appears in Section 5.1, highlighted in yellow. Table 2 is described in Section 5.2 and 5.3.

- b. You must also clearly state whether you have explored a range of parameterizations and discuss its outcome.

The text of the paper has been widely extended to include the effects of modeling techniques and parameterizations, for instance regarding the sediment processes simulated by using a number of parameters. Moreover, the consequences of using a morphological factor to speed up computations have been discussed (Section 5.3, highlighted in yellow). This led to the suggestion to reduce the morphological factor in the future (Chapter 8).

- c. You use a depth averaged version of the hydrodynamic model so you must discuss the interest of coupling it to a 3D sediment conservation equation and how you handle the vertical coordinates?

The sediment conservation in the model is not 3D. The vertical structure of the soil that arises from the computations is the result of storing the bed level changes together with the characteristics of the sediment that is deposited during every time step. So the model is purely 2D in its hydrodynamic and morphodynamic part. Thanks to your question we realized how badly the model described in the first version of the paper, so we have improved the description of the model (Section 5.1 at the end).

- d. Where does eq2 come from?

The description of the model in this part was not clear, because we showed a 3D advection-diffusion equation, whereas the model is 2DH (depth-averaged). In the 2D model the hindered settling effect is not accounted for. So this part has been removed and the story completely re-written (Section 5.1, Equations 1 and 3). Sorry for the confusion.

- e. What are the values of each and every parameter you describe in eq (2-4) and how where they quantified (this is only partly answered in the calibration sections?)

Please read our reply to the previous question first. All the parameters described in the 2D Equations (1 to 3) are computed, except for the following parameters which are input parameters to the model, adjusted during the calibration phase:

#	Physical parameter	The value used	Remark
1	Horizontal eddy diffusivity	10 (m ² /s)	
2	C _{soil} (reference density of hindering settling)	1600 (kg/m ³)	For both sediment
3	W _{s,0} (the settling velocity of the sediment particle)	0.005 (mm/s)	For cohesive sediment only
	τ _c (critical shear stress for erosion)	1.0 (N/m ²)	For cohesive sediment only
	M (entrainment coefficient)	2 (mg/m ² /s)	For cohesive sediment only

(7) Comment: 5.2 hydrodynamic calibration

You have a bathymetric survey in 2009. The fact that you need to modify it to calibrate the hydrology presents a problem either for the model or the bathymetric data. You should show the calibration result with the measured topography for comparison purposes and discuss this issue in more details

The 2009 bathymetric survey was used in the model because the only measurement that can be used for calibration are available in 2009 and 2010. Therefore, the hydrodynamic calibration was conducted using the data of 2009 (the survey, the inflow and the reservoir water level). During the calibration, we found an incorrect water depth interpolation, at a few locations, during bed-topography generation by the model. This incorrectness created inaccuracies in the the water levels at Famaka. Therefore, manual adjustment according to the samples was executed. The experience gained from this treatment was applied to the other topographical maps as well. This procedure has been described in the new paper version (Section 5.2).

The calibration for the hydrodynamic part only was carried out to ensure that the model simulates the hydrodynamics well.

(8) Comment: 5.3 morphodynamic calibration

Lines 9-13 ??? Can you explain this procedure ? Written this way it looks obscure. The density is small, what is the petrology of the silts?

The adoption of a morphological factor to speed up the computations and its consequences for the results have been extensively described in Section 5.3.

The small density assigned to deposited silt ($1,200 \text{ kg/m}^3$) corresponds to a porosity of 0.55; the density imposed to the sand deposits ($2,000 \text{ kg/m}^3$) corresponds to a porosity of 0.25. Both values of the porosity are realistic.

(9) Comment: 6 coring

Given the poor performance of the model to what level of confidence do you assess coring sites?

We could only excavate four trenches and our results are much affected by this. However, sand was clearly present, from fine to medium, and this was systematically so in all coring sites. Chapter 7 has been much extended, including some analysis of the discrepancies between model and field data, considering that the model did not predict so much sand to be deposited at the coring locations.

Thanks to you and the other reviewer we believe that our paper has been improved. We have better described the model and the modeling techniques, but the most important additional parts relate to the analysis of why the model has failed in the description of sand transport and deposition inside the reservoir. We also added some recommendations for the future.

Modelling of sedimentation processes inside Roseires Reservoir (Sudan)

Amgad Y. A. Omer^{1,2}, Yasir S. A. Ali^{1,3}, J.A. (Dano) Roelvink^{1,4}, Ali Dastgheib¹, Paolo Paron¹ and Alessandra Crosato^{1,5}

[1] UNESCO-IHE, Westvest 7, 2601 DA Delft, the Netherlands, and

[2] Dams Implementation Unit of Ministry of Water Resources and Electricity, P. O. Box 12843, Mashtal Street, Riyadh District, Quarter No. 16 Khartoum, Sudan.

[3] Ministry of Water Resources and Electricity, Hydraulic Research Station, Wad Madani, Sudan.

[4] Deltares, Rotterdamseweg 185, Delft, the Netherlands.

[5] Delft University of Technology, Faculty of Civil Engineering and Geosciences, Delft, the Netherlands.

Correspondence Author: Yasir Salih Ahmed Ali, Ministry of Water Resources and Electricity, Hydraulics Research Center, P.O.Box 318, Wad Medani, Sudan.

E-mail: yasir_hrs@hotmail.com, Tel +249916780223, Fax +249511859700.

Abstract

Roseires Reservoir, located on the Blue Nile River, in Sudan, is the first trap to the sediments coming from the vast upper river catchment, in Ethiopia, suffering from high erosion and desertification problems. The reservoir lost already more than one third of its storage capacity due to sedimentation in the last four decades. Appropriate management of the eroded soils in the upper basin could mitigate this problem. In order to do that, the areas providing the highest sediment volumes to the river have to be identified, since they should have priority with respect to the application of erosion control practices. This requires studying the sedimentation record inside Roseires Reservoir, with the aim of identifying when and how much sediment is deposited, as well as its source. This paper deals with the identification of deposition time and soil stratification inside the reservoir, based on historical bathymetric data, numerical modeling and newly acquired soil data. The remoteness of the study area and the extreme climate result in expensive and difficult coring campaigns. For this, these activities need to be optimized and coring locations selected beforehand. This was

done by combining bathymetric data and the results of a depth-averaged morphodynamic model recording the vertical stratification in sediment deposits. The model allowed recognising the areas that are potentially neither subject to net erosion nor to bar migration during the life span of the reservoir. Verification of these results was carried out by analysing sediment stratification from the data collected during the subsequent field campaign.

1 Background information

1.1 The Blue Nile River

The Blue Nile is the main tributary of the Nile River. It originates at the outlet of Lake Tana and flows for nearly 900 km through Ethiopia, before reaching the Sudanese border. In Ethiopia, the Blue Nile has 14 major tributaries (Fig. 1a), which represent the majority of the estimated annual flow of the river that is 46.2 billion m³/year. Here, the river falls from 1800 m above sea level at Tana to about 490 m above sea level at the Sudan border, which gives an averaged longitudinal slope of 1.5 m/km (Fig. 1 b). The upper basin suffers from high erosion problems due to intensive land use and upper catchment desertification and delivers huge quantities of sediment to the river system (Ayalew and Yamagishi, 2004). After leaving Ethiopia, the Blue Nile runs through Sudan for about 735 km to Khartoum, where it joins the White Nile to form the Nile River. Presently, the Blue Nile waters encounter two dams: the Roseires Dam and the Sennar Dam (Fig. 1 a), both in Sudan, but a new dam is currently under construction in Ethiopia, the Grand Renaissance Dam, and other dams are planned.

The slope from the Ethiopian border to Khartoum is one order of magnitude milder than in the Ethiopian side, only 15 cm/km (Abdelsalam and Ismail, 2008). The Dindir and Rahad rivers join the Blue Nile downstream of Sennar Dam in Sudan, contributing with an average annual flow of 4 billion m³/year together.

The flow of the Blue Nile reflects the seasonality of rainfall over the Ethiopian highlands, which can be distinguished in wet season, from July to October, with maximum flow in August-September and dry season, from November to June. Consequently, the annual Blue Nile hydrograph at the Ethiopian Sudanese border has a bell-shape pattern. The daily flow of the river fluctuates between 10 million m³ in April to 500 million m³ in August with a ratio of 1:50 (Awulachew et al., 2008).

1.2 Roseires Reservoir

Roseires Reservoir is located in Sudan 550 km southeast of Khartoum, near the border with Ethiopia (Fig. 1a). It is one of the oldest reservoirs in the basin, since the dam was finalised in 1966 (Fig. 2). This reservoir plays an important role for the economy of Sudan, since it provides hydropower, water for irrigation and flood control. The maximum length of the reservoir is about 80 km and the wet area surface is up to 290 km². The total storage capacity was 3 billion m³ (Bashar and Eltayeb, 2010) but in the mean time the reservoir has lost 40% of this storage capacity due to sediment deposition (Ali 2014). To limit sedimentation (Sloff, 1997), the gates are kept to the minimum level (open) in the wet season and are raised to the maximum level one month before the end of the high flow season and kept so during the dry season (Hussein et al., 2005). During the gate opening period the water drops by approximately 13 m and the area surrounding the channel becomes dry. Dredging is executed every year in front of the power intake. Dredged sediment is dumped in front of the deep sluice gates to be transported away during the flood season when all the dam gates are open. The process is generally carried out before the flood season (Bashar and Eltayeb, 2010).

To increase the storage capacity of the reservoir, the dam has been recently heightened by 10 metres (in 2013). Before heightening, the full supply level was 481 m above sea level (Irrigation Datum) and the minimum supply level of the power generation during flood season was 467.6 m above sea level (Irrigation Datum) (Hussein et al., 2005). The bed of the reservoir is cut through by a 10 m deep channel.

2 Reservoir sedimentation from bathymetric data

The reservoir was surveyed in 1976, 1985 (DEMAS, 1985), 1992 (Gismalla, 1993), 2007 (Abd Alla and Elnoor, 2007) and 2009 (Omer, 2011). The bathymetric surveys prior to 2009 do not cover the upstream river reach up to ElDeim station, as well as the left and right wings of the reservoir (Fig. 3). The bathymetry was measured using an Acoustic Doppler Current Profiler (single beam) and eco-sounders for the wet areas and a differential GPS and survey levels for the temporarily dry areas along specific transects at intervals of 2-5 km or more in most of the surveys. This low resolution created uncertainty in the generated topographical maps. Moreover, the assessment of the changes in bed elevation was made difficult by the different coordinate systems used and by inaccuracies in the horizontal coordinates. All data

were therefore checked, corrected and transformed using the Irrigation Datum as the reference vertical level.

The local changes of bed level were obtained by comparing the bathymetric data of 20 sections surveyed in 1985, 1992 and 2007. The resulting temporal variations in storage capacity of Roseires Reservoir are given in Table 1. By subtracting the bed topographies derived from the measured bathymetries, the total storage volume lost in the two periods 1985-1992 and 1992-2007 was quantified in 146 and 238 million m³, respectively.

The areas with net deposition or erosion were identified by subtracting the bed topography in the two time intervals described above: 2007 minus 1992 and 1992 minus 1985.

3 Available hydrodynamic and sediment data

Most data were provided by the Ministry of Irrigation and Water Resources (MoIWR) and by the Dams Implementation Unit of the Ministry of Dams and Electricity, Sudan. Fig. 2 shows the location of the measuring stations for water levels and sediment concentration inside Roseires Reservoir.

ElDeim gauging station for water level, discharge and sediment concentration is located near the Sudan-Ethiopia border. It was established in 1962 during the construction of the dam 110 km upstream along the river and 85.5 km air distance (Fig. 2). The station is situated in a deep rock gorge, which is supposed to provide a very stable control. However, in the last three decades ElDeim station has deteriorated and not working properly (Ahmed and Ismail, 2008). Water level, discharge and sediment concentration are also available at Famaka at the reservoir inlet, Wad Almahi inside the reservoir and Wad Alies, just downstream of the dam.

The concentration of suspended solids was measured during the flood season at ElDeim on a daily basis during the last four decades. The data show a high variability in suspended solids concentrations from year to year and substantial differences between the rising limb and the falling limb of the flood curve (Hussein et al., 2005; Ahmed and Ismail, 2008; Billi and el Badri Ali, 2010; Ahmed et al. 2010). Considering the long-term character of the investigation, to represent the historical inputs of suspended solids during the high-flow seasons we derived the averaged values of suspended solids concentrations from the collected data for three periods:

the 1970-1980s, the 1990s and the 2000s. For the low-flow seasons, due to lack of historical data, we adopted the averaged sediment concentration of 0.024 kg/m^3 that we measured during a field campaign in 2011.

The mean diameter of suspended sediment is $18.5\mu\text{m}$ and $22\mu\text{m}$ at Wad Almahi and Wad Alies, respectively. Silt is the dominant type of sediment in suspension and it represents more than 80% of the samples. Sand represents about 15% of the suspended sediment inside the reservoir (at Wad Almahi) and 10% of the suspended sediment downstream of the dam (at Wad Alies), as shown in Fig. 4. The analysis of the bed material (Omer, 2011) shows that at some locations sediment contains up to 30% of silt and clay. Averaging results in a D_{50} of $1,200 \mu\text{m}$ upstream of Famaka and in a D_{50} of $140 \mu\text{m}$ just upstream of the dam.

4 Methodology

Deposition time and soil stratification inside the reservoir are assessed based on the historical bathymetric data, numerical modeling and newly acquired soil data. The study is based on the hypothesis that the alternated stratification of sand and silt reflects the alternation of wet and dry years, respectively.

The analysis of the sediment deposited in the reservoir, however, requires extensive field campaigns, whereas environmental conditions and economical issues limit the possibility to go to the field. For this, field campaigns had to be optimized beforehand.

With the aim of identifying the most promising sampling areas to investigate soil stratification in the reservoir, we combined the analysis of bathymetric data and the results of a morphodynamic model. Data alone allow identifying areas characterized by net sedimentation, but these areas might experience periods of erosion in which part of the layers are lost. Instead, by recording erosion and deposition during the development of the bed topography, the model would allow recognizing the best areas. Another advantage of using a numerical model lies in the possibility of better analyzing the sedimentation process in Roseires Reservoir, especially if data are scarce and not always reliable, particularly regarding the time evolution.

We adopted a physics-based model that allowed to obtain vertical and horizontal sediment sorting inside the reservoir. The morphodynamic model was constructed using the Delft3D software. The set up of the model required two steps: 1) the development of a 2D depth-averaged hydrodynamic model; and 2) the development of

a 2D morphodynamic model considering two types of sediments: silt and sand, according to the two types of sediment transported by the Blue Nile River.

5 Modeling

5.1 Model description

Lesser et al. (2004) extensively describes the open-source Delft3D code which is applied in the current study (see also: <http://oss.deltares.nl/web/delft3d>).

The hydrodynamic part of the model is based on the 3-D Reynolds-Averaged Navier–Stokes (RANS) equations for incompressible fluid and water (Boussinesq approximation: Boussinesq, 1903). The closure scheme for turbulence is a k – ϵ model, in which k is the turbulent kinetic energy and ϵ is the turbulent dissipation. The equations are formulated in orthogonal curvilinear co-ordinates. The set of partial differential equations in combination with the set of initial and boundary conditions is solved on a finite-difference grid.

We used a 2-D depth-averaged version of the model with an appropriate parameterization of two relevant 3-D effects of the spiral motion that arises in curved flow (Blanckaert et al., 2003). First, the model corrects the direction of sediment transport through a modification in the direction of the bed shear stress, which would otherwise coincide with the direction of the depth-averaged flow velocity vector. Second, the model includes the transverse redistribution of main flow velocity due to the secondary-flow convection, through a correction in the bed friction term. Taking into account these 3-D effects becomes important not only in curved channels, but also in straight channels with bars.

The morphodynamic part of the model simulates the processes of sand (capacity-limited transport) and silt (supply-limited transport) separately. For capacity-limited sediment transport, the evolution of the bed topography is computed from a sediment mass balance equation and a sediment transport formula (Exner approach). A number of capacity-limited transport formulas are available, such as Meyer-Peter and Muller's (1947), Engelund and Hansen's (1967) and van Rijn's (1984). The model accounts for the effects of gravity along longitudinal and transverse bed slopes on bed load direction (Bagnold, 1966; Ikeda, 1982).

For supply-limited transport (fine sediment travelling in suspension), the evolution of the bed topography is computed from the sediment mass balance and an advection-

diffusion formulation describing the temporal and spatial evolution of suspended solids concentration, coupled to two formulas describing the entrainment and deposition processes. The adopted 2D (depth-averaged) advection-diffusion equation is:

$$\frac{\partial c}{\partial t} + \frac{\partial uc}{\partial x} + \frac{\partial vc}{\partial y} = \frac{\partial}{\partial x}(\varepsilon_{s,x} \frac{\partial c}{\partial x}) + \frac{\partial}{\partial y}(\varepsilon_{s,y} \frac{\partial c}{\partial y}) \quad (1)$$

where c is the mass (depth-averaged) concentration of the fine sediment fraction (kg/m^3) and u and v are the flow velocity components in x and y direction, respectively (m/s). The velocity and eddy diffusivity ($\varepsilon_{s,x,y}$) components are obtained from the hydrodynamic model.

The following formula (Ariathurai and Arulanandan, 1978; Partheniades, 1964) describes the entrainment of fine sediment from the bed:

$$E = M \left(\frac{\tau - \tau_c}{\tau_c} \right) \quad (2)$$

where E is the erosion flux ($\text{kg/m}^2/\text{s}$), τ is the bed shear stress (N/m^2) and τ_c is the critical shear stress for erosion (N/m^2). M is a coefficient quantifying the erosion rate ($\text{kg/m}^2/\text{s}$). The following formula describes the deposition rate:

$$D = Cw_s \quad (3)$$

in which D is the deposition rate ($\text{kg/m}^2/\text{s}$), C is the sediment concentration (depth-averaged) (e.g. Montes et al., 2010) and w_s is the fall velocity of suspended solids (m/s). It is assumed that deposition occurs only if the bed shear stress does not exceed the critical shear stress for deposition, τ_d (N/m^2).

For the description of the soil processes, the model records the bed level changes in vertical direction with time together with the composition of the deposited sediment, according to an adapted version of Hirano's (1971) bed layer model (Blom, 2008). This permits studying the evolution of the vertical stratification of sediment deposits.

5.2 Hydrodynamic model: setup, calibration and validation

The 2D depth-averaged model was built to cover the Reservoir area from the dam to ElDeim, 30 km upstream of the end of the reservoir (about 110 km in total). The reservoir shape is rather complex, as shown in Fig. 2. Consequently, the computational curvilinear grid size is variable, ranging between 25 to 280 m (Fig. 6). The upstream boundary condition was represented by the daily discharge time series measured at ElDeim. The downstream boundary condition was represented by the corresponding water levels measured at Wad Almahi and by the dam outflow discharges.

The selection of the simulation time step depends on several parameters, such as the grid size of the model, the water depth, the required accuracy and the stability of the model during simulation. The Courant number (C_r) is defined by:

$$C_r = \frac{\Delta t \sqrt{gh}}{\{\Delta x, \Delta y\}} \quad (4)$$

In general, C_r should not exceed the value of ten (Delft3D-manual, 2010). For the hydrodynamic model and the selected schematization of the grid cells, the time step used is 30 s and the value of C_r varies in space and time. The values of other numerical parameters adopted in the model coincide with the default values of the Delft3D software.

During the model setup phase, inaccuracies due to the large size of the computational grid cells were compensated by manual adjustments of topographic levels, ensuring that the Thalweg elevation in the model is close to the measured one.

The hydrodynamic model was calibrated on the 2009 water levels measured at Famaka, a measuring station located inside the reservoir, about 80 km upstream of

the dam (Fig. 2). The chosen values of the calibration parameters and the closure coefficients for the k - ε model are given in Table 2. In particular, the bed roughness, resulted in a Chézy coefficient of $80 \text{ m}^{1/2}/\text{s}$. Fig. 7 (a) shows the results of model calibration.

The hydrodynamic model was validated using the 2010 daily discharge time series measured at ElDeim, as upstream open boundary condition, dam outflow and the water levels measured at Wad Almahi (inside the reservoir). Fig. 7 (b) shows the results of model validation.

5.3 Morphodynamic model: setup, calibration and validation

The hydrodynamic model was then used to set up the morphodynamic model, with the aim to simulate sediment deposition and erosion inside the reservoir during the two periods 1985-1992, and 1992-2007. The model was calibrated and validated on the measured bed level changes in these two periods derived from the bathymetric data. There were no data available on soil stratification. The hydrodynamic boundary conditions were the time series of monthly inflow and outflow discharges and averaged water levels inside the reservoir.

Due to the large number of computational cells, related to the size of the reservoir, and to the complexity of the processes to be simulated, such as 2D hydrodynamics, bed load and suspended load transport, soil erosion and sediment deposition, bed level changes and storing of the characteristics of deposited material, the morphodynamic computations were excessively time consuming. To limit the duration of each computational run to a couple of weeks, the morphodynamic model was speeded up using the morphological factor introduced by Roelvink (2006). We adopted a morphological factor equal to 30, to represent the morphological changes occurring in one month by simulating one single day (hydrodynamically). This is obtained by multiplying the corresponding morphological changes by a factor of 30. The approach creates a water balance problem in the reservoir, since the hydrodynamic part could not represent the behaviour of one month. To respect the balance, water was added to or subtracted from the reservoir during the computations, which could be done only in a distributed way, to be applied to the wet surface of the reservoir, similar to rain and evaporation. The relation surface-elevation was derived from the bathymetric data and then used for this purpose (Fig. 5). This method allowed respecting the water balance

and the water levels in the reservoir, but not the flow velocity distribution inside the reservoir, which suffered of inaccuracies. These were mainly due to the gradual increase/decrease of water discharge along the reservoir and were particularly affecting the filling in and flushing times.

Dredging was implemented as yearly operation. The upstream input of suspended sediment concentrations during high flows was the corresponding averaged values derived from the measured data. Suspended sediment input during the low flow season was kept constant and equal to the measured one.

The model was calibrated on the period 1985-1992. This period was selected due to the availability of topographical surveys. This means that the model was run for 7 years with the required input data starting from the bed topography measured in 1985. The final result of the model was then compared with the measured topography of 1992. The model parameters were tuned until the simulated topography compared to the measured one in a satisfactory way.

Given the large variety of sediments settling in the reservoir and the necessity to consider only two components (sand and silt), the transport formula for sand having an averaged diameter of 700 μm , the fall velocity, the critical shear stress for erosion and the erosion speed of fine suspended solids were all used as calibration parameters (Table 2).

The transport formula that gave the best results for the sand component was van Rijn's (1984). The optimized fall velocity of the fine suspended solids resulted in 0.005 mm/s and the critical shear stress for the erosion of deposited silt in 1 N/m^2 . For bed shear stresses above this value the bed of the reservoir eroded with an erosion rate of $2 \text{ mg/m}^2/\text{s}$. In natural systems, the erosion rate is a function of bed density (consolidation) and bed shear stress. However, consolidation of sediment deposits is not taken into account in the model. This means that all densities are prescribed initially and kept constant in time. We applied a dry-bed density of $1,200 \text{ kg/m}^3$ for the deposited silt (porosity = 0.55), and of $2,000 \text{ kg/m}^3$ for sand (porosity = 0.25). In the model, the value of the dry density does not have any influence on the erosion rate, but it has some influence on the bed-level changes (the smaller the imposed dry density is, the larger the change in volume due to the presence of the pores between the sediment particles).

The critical shear stress for deposition resulted in $1,000 \text{ N/m}^2$. Below this value, any particle was free to deposit according to its fall velocity and depending on the computed bed shear stress.

Fig. 8 shows the measured and simulated cross-sections 18 and 19B (10.8 km and 15.4 km upstream of the dam). The model does not provide accurate results at this level of detail. Computed section 18 shows that the model fails to simulate the main channel shift (compare measured and simulated 1992 topography). The same applies to Section 19B. This might be due to the relatively large grid size and the distance of the measured cross-sections (2-5 km) which does not allow for proper reproduction of curved flow effects inside the main channel.

Fig. 9(a) shows the measured difference in bed topography and Fig. 9(b) the simulated difference 1992-1985. In the figures, the ellipses show the areas for which the bed topography of 1985 and 1992, being unknown, was put equal to the bed topography of 2009. These areas should therefore not be considered, although they might have influenced the bed level changes in other areas. By comparing simulated with measured differences in bed elevation, it can be observed that the upstream part (1), subjected to deposition, has the same deposition pattern, but a smaller deposited volume, in the simulation. Some eroded areas (2) can be recognized also in the simulation, especially the area closer to the dam and the narrow area more upstream.

The total computed cumulative deposited volume of sediment in the period 1985-1992 is 188 million m^3 , which is 29% larger than the measured volume (146 million m^3 , from Table 1). Based on this we considered the results of the calibration as satisfactory.

The model was then validated on the developments occurred in the next 15 years, from the end of 1992 to the end of 2007. The runs started with the bed topography 1992. The results representing the bed topography after 15 years were compared to the measured bed levels in 2007. The simulated morphological changes inside Roseires Reservoir show significantly higher deposition rates than the measured ones. The computed total cumulative sediment deposit in this period is 567 million m^3 , which is more than double of the measured 238 million m^3 (Table 1). To analyze the implications of this overestimation at the cross-sectional scale, we compare the measured and simulated sections 18 and 19B in Fig. 10. The simulated section 18 in 2007 shows a deposition of 2-2.5 m with respect to section 18 in 1992, which is larger

than the measured one. In particular, the model does not correctly reproduce the main channel shift inside the reservoir at section 19B.

We believe that the unavailability of good field data reflects on the model accuracy and output reliability. In this study, data were not available in sufficient detail, and were limited in terms of quality and extent. For instance, the cross-sections measured during the bathymetric surveys of 2009 are 2 to 5 km far from each-other and the surveys do not cover the entire length of the reservoir. This creates inaccuracy to prepare the reservoir bed topography considering the length of Roseires Reservoir (80 km) and its meandering shape. The relatively large grid size adopted in the model adds to this. The combination of poor data and model accuracy resulted in the smoothing down of the bed topography differences, which is particularly impacting on the simulated channel inside the reservoir. The simulated flow velocity is more uniform than in reality and remarkably smaller in the channel. Smaller velocity in the channel results in excessive sedimentation of the sand component in the upstream part of the reservoir, lack of sand in the deposits more downstream, higher deposition rates of the silt component, less efficient sediment flushing in the model than in reality. Since the channel becomes more important with time as reservoir sedimentation progresses, this effect is more important for the validation period than for the calibration period. This might explain the increased overestimation of sediment deposition for the validation period.

The discrepancies between model and measurements could also be caused by an overestimation of the sediment inputs. In particular, the suspended solids concentrations for the years 2000's seem to be overestimated by the adopted averaged value.

6 Identification of promising coring areas

One important goal of the modeling study was the identification of the most promising sampling locations to study soil stratification. These locations should fulfill the following conditions: 1) easy accessibility; 2) absence of bed erosion; 3) absence of bar movement, destroying soil stratification; 4) recognizable soil stratification.

Two areas were selected for the sampling, as shown in Fig. 11, based on the absence of erosion and of bar migration in the model outputs.

Area 1. Fig. 12 shows the vertical profiles of deposition at Area 1. In Fig. 12 (a), the solid lines represent the final bed levels of 1985, 1988 and 1991. In Fig. 12 (b), the solid lines represent the final bed levels of 1992, 1995, 1998, 2001, 2004 and 2007. In areas characterized by the absence of bed erosion, the lowest solid line represents the first year, whereas the top line represents the final year of the computation. In Area 1, according to the model, deposition always occurs at the right side of the reservoir, from 0 m to 250 m from the right bank. Erosion occurs due to channel shift in the middle of the reservoir. The last 200 m at left side of the reservoir, from 1500 m to 1700 m, are again characterized by deposition only. The dominant deposited sediment in 1986 (dry year) is sand. Sand content is higher in the period 1985-1992 (Fig. 12 (a)) than in the following 15 years (Fig. 12 (b)). The general trend in the years 1989, 1990, 1991 and 1992 is deposition of coarser sediment in the deepest area (main channel). Deposition and stratification occur at the sides of the reservoir. These areas become dry at the end of the dry season, are always characterized by deposition and are therefore promising coring areas.

Area 2. According to the model, the left side of this section is subject to deposition only, for approximately 3 km. In this area, the reservoir is relatively wide. Most of sediment deposited in this section is silt with only a minor percentage of sand. Stratification is less visible or absent and for this Area 2 seems less suitable than Area 1 for coring.

7 Model verification based on soil stratification data

A subsequent field campaign was carried out in the summer 2012 in the areas identified by the model. We visited those areas during the rainy season, when the reservoir gates are open and the water level is the lowest. This allowed reaching zones that are normally submerged. The central channel, however, was not reachable and sampling was carried out only in the areas that had become dry on the right or left bank. In Area 1, about 45 km upstream of the dam, the reservoir width is 1.5 km, whereas in Area 2, 25 km upstream of the dam, the reservoir width is 4 km. The larger width allowed covering a wider transect, but due to a number of logistic constraints during the field campaign we were able to excavate only four trenches. Three trenches were excavated in Area 2 and a fourth trench was excavated in Area 1. The characteristics and locations of the four trenches are summarized in Table 2 and shown in Fig. 13.

Sampling in these areas allowed studying the granulometric characteristics of the deposited sediment and validating the model results in terms of soil stratification. The analysis of the sediment showed that indeed, at least in the selected areas, the reservoir soil is stratified. However, the layers are not distinguishable from alternations of sand and silt, but from alternations of coarse and fine sand. These alternations are visible from the vertical profile of the D_{90} of the sediment (Fig. 14). This important difference between model and field data can be attributed to systematic underestimation of the flow velocities inside the reservoir, particularly inside the channel, where most sand is transported downstream. This is most probably due to the difficulty to guarantee the water balance (due to the adoption of a morphological factor) and to reproduce the channel excavated within the reservoir soil (due to low model and data resolution). Both morphological factor and poor resolution were inevitable, though, given the long simulation times (weeks) and the data available for the study. Underestimation of flow velocity results in higher sedimentation rates and in sand being deposited in the upstream part of the reservoir (delta formation: Fan and Morris, 1992; Kostic and Parker, 2003 a and b).

No signs of soil erosion could be detected from the analysis of the trenches. This means that the model was successful in identifying the areas in which no soil erosion has occurred.

Sediments are believed to become finer farther from the central channel in transverse direction, where the flow velocity (during high water) is smaller, and in downstream direction, due to selective deposition in the reservoir, the coarser material being deposited in the upper parts. However, clear sediment sorting trends cannot be observed from the field data, neither in transverse direction nor in longitudinal direction. We believe that this is due to the limited number of excavated trenches. Sedimentation strongly depends on local hydrodynamic conditions and for this a general sorting trend can only be detected with a large number of spatially distributed coring locations.

8 Conclusions

The most promising coring areas inside Roseires Reservoir were selected by combining bathymetric data analysis with the results of a 2D morphodynamic model including horizontal and vertical sorting. The model allowed studying the contribution of two sediment types, sand and silt, both transported by the Blue Nile into the

reservoir. The model set up was based on the **hypothesis** that sand is deposited during high flows, whereas fine material, mainly originating from upper catchment erosion, is deposited during low flow periods. This would create soil stratification inside the reservoir, allowing for the recognition of specific wet or dry years. The model, with recorded bed level changes and soil composition in vertical direction, shows vertical stratification in the reservoir soil at several cross-sections. Two of them were selected as the best areas for analyzing the sedimentation process in the reservoir.

The results of the subsequent field campaign carried out in the summer 2012, show clear **soil stratification** at the four trenches excavated in the selected areas, but layers are mainly distinguishable from the presence of coarse and fine sand rather than from alternations of sand and silt. Coarse sand was mainly deposited there during distinguishable wet years, which allowed recognizing the progression of sediment deposition in the reservoir from **the collected soil data**.

Sand appears to be transported and deposited in the reservoir much further downstream than the model predicts. This can be explained by systematic underestimation of the flow velocity in the reservoir during high flows. The cause seems to lie in the adoption of a morphological factor to speed up the computations leading to inaccuracies in the flow velocity estimation and in the poor resolution of data and model, resulting in a more uniform bed topography and flow velocity, leading to smaller velocity in the central channel where sand is transported downstream.

The discrepancies between model and measurements could also be due to an overestimation of the sediment inputs. In particular, the suspended solids concentrations for the years 2000's seem to be overestimated by the adopted averaged value. For this reason, suspended solids concentrations should be carefully measured in the future. In particular, more measurements are required during the low-water season, at least for modeling purposes.

To implement the model in a more reliable way in the future, it is suggested to reduce its cell size, to reduce or eliminate the morphological factor and to perform more accurate bathymetric surveys, preferably with a side-scan sonar. If computational cell size reduction is not feasible, due to unacceptably long computational times, the suggestion is to nest the model with smaller cells in the central area occupied by the channel.

Notwithstanding these limitations, the model allowed recognizing two appropriated coring areas, where the soil had never been eroded and was indeed stratified. Moreover, the model allowed analyzing the sedimentation process in the reservoir with a level of detail that would not have been possible by solely analyzing the available data, allowing for data correction at several locations of which the horizontal coordinates were uncertain.

Acknowledgements

The study was carried out as a project within a larger research program called “In search of sustainable catchments and basin-wide solidarities in the Blue Nile River Basin”, funded by the Foundation for the Advancement of Tropical Research (WOTRO) of the Netherlands Organization for Scientific Research (NWO) and UNESCO-IHE. The authors are grateful to the Ministry of Water Resources and Electricity, Hydraulic Research Station, Wad Madani, and the Dam Implementation Unit, Khartoum, Sudan, for providing data free of charge. The authors wish to thank Dr. Mick van der Wegen, Dr. Kees Sloff for their helpful advices in the modeling phase. The authors wish to thank Mohamed Osman and Yasir Abo ElGasim for their helpful support during the field work.

References

Abd Alla, M.B. and Elnoor, K.: Hydrographic Survey of Roseires Reservoir, Ministry of Irrigation and Water Resources, Khartoum, Sudan, Khartoum, 2007.

Ahmed, A.A. and Ismail, U.H.A.E.: Sediment in the Nile River system. Consultancy Study requested by UNESCO and International Sediment Initiative (ISI), Khartoum, Sudan, 2008.

Ahmed, A.A., Ibrahim, S.A.S., Ogembo, O., Babikir, I.A.A., Fadul, H.M., Ibrahim, A.A. and Crosato, A.: Nile River bank erosion and protection, Hydraulic Research Institute, Cairo, Egypt, 2010.

Ali Y.S.A.: The impact of soil erosion in the Upper Blue Nile on downstream reservoir sedimentation. Ph.D. Thesis, Technical University of Delft, the Netherlands, 17 p., 2014, ISBN 978-1-138-02742-8 (Taylor & Francis Group).

Ariathurai, R. and Arulanandan, K.: Erosion rates of cohesive soils. Journal of the Hydraulics Division, 104, 279-283, 1978.

Awulachew, S.B., McCartney, M., Steenhuis, T.S. and Ahmed, A.A.: A review of hydrology, sediment and water resource use in the Blue Nile Basin. International Water Management Institute, Addis Ababa, Ethiopia, 2008.

Ayalew, L. and Yamagishi, H.: Slope failures in the Blue Nile basin, as seen from landscape evolution perspective. *Geomorphology*, 57, 95-116, 2004.

Bagnold, R.: An approach to the sediment transport problem from general physics: US Geol. Survey Professional Paper 422-I, Washington, 1-37. 1966.

Bashar, K.E. and Eltayeb, A.: Sediment Accumulation in Roseires Reservoir. Nile Basin Water Science and Engineering Journal, 3, 46-55, 2010.

Billi, P. and el Badri Ali, O.: Sediment transport of the Blue Nile at Khartoum. *Quaternary International*, 226, 12-22, 2010.

Blanckaert, K., Glasson, L., Jagers, H.R.A. and Sloff, C.J.: Quasi-3D simulation of flow in sharp open-channel bends with equilibrium bed topography, in: proc. RCEM 2003, 1-5 Sept. 2003, Barcelona, Spain, eds. A.Sanchez-Arcilla & Bateman A., IAHR, Vol. I, 652-663, 2003.

Blom, A.: Different approaches to handling vertical and streamwise sorting in modelling river morphodynamics. *Water Resources Research*, 44, W03415, doi:10.1029/2006WR005474,2008.

Boussinesq, J.: *Theorie analytique de la chaleur*. Gautier Villars, 2, Paris, 1903 (in French).

DEMAS (Dredging, Engineering and Management Studies): Roseires Reservoir Survey - Blue Nile, Ministry of Irrigation and Hydropower, Khartoum, 1985.

Engelund, F. and Hansen, E.: *A Monograph on Sediment Transport in Alluvial Streams*, Technisk Vorlaq, Copenhagen, Denmark, 1967.

Fan, J., and Morris, G.: Reservoir sedimentation. I: Delta and density current deposits. *Journal of Hydraulic Engineering, ASCE*, 118(3), 354-369, 1992.

Gismalla, Y.A.: *Bathymetric Survey of Roseires Reservoir*, Ministry of Irrigation and Water Resources, Wad-Madani (Sudan), 1993.

Hirano, M.: River bed degradation with armouring. *Transactions of Japan Society of Civil Engineering*, 3, 194-195, 1971.

Hussein, A.S., Bashar, K.E., ElTahir, E.T.O., Fattah, S.A. and Siyam, A.M.: *Reservoir Sedimentation, Nile Basin Capacity Building Network (NBCBN)*, Khartoum, Sudan, 2005.

Ikeda, S.: Lateral bed load transport on side slopes. *Journal of the Hydraulics Division*, 108 (11), 1369-1373, 1982.

Kostic, S., and Parker, G.: Progradational sand-mud deltas in lakes and reservoirs. Part 1: Theory and numerical model. *Journal of Hydraulic Research*, 41(2), 2003a.

Kostic, S., and Parker, G.: Progradational sand-mud deltas in lakes and reservoirs. Part 2. Experiment and numerical simulation. *Journal of Hydraulic Research*, 41(2), 2003b.

Lesser, G.R., Roelvink, J.A., van Kester, J.A.T.M. and Stelling, G.S.: Development and validation of a three-dimensional morphological model. *Coastal Engineering*, 51, 883-915, 2004.

Meyer-Peter E. and Müller R.: Formulas for bed load transport, in: *Proceedings of the 2nd IAHR Congress, Stockholm, Sweden*, 2, 39-64, 1948.

Montes, A.A., Crosato, A. and Middelkoop, H.: Reconstructing the early 19th century Waal River by means of a 2D physics-based numerical model. *Hydrological processes*, 24, 1-15, Wiley InterScience DOI: 10.1002/hyp.7804, 2010.

Omer A.Y. A.: Sedimentation of sand and silt in Roseires Reservoir: vertical and horizontal sorting with time. MSc thesis (WSE-HERBD.11.08), UNESCO-IHE, Delft, the Netherlands, 2011.

Partheniades, E.: A summary of the present knowledge of the behavior of fine sediments in estuaries. Technical Note no 8, Hydrodynamics Lab, Massachusetts Institute of Technology, Cambridge, MA, June 1964.

Roelvink, J.A.: Coastal morphodynamic evolution techniques. *Journal of Coastal Engineering*, 53, 177-187, 2006.

Sloff, C.J.: Sedimentation in reservoirs. Ph.D. Thesis, Technical University of Delft, the Netherlands, 269 p., 1997 (also in: *Communications on Hydraulic and Geotechnical Engineering*, Technical University of Delft, Report 97-1, ISBN 90-9010530-1).

Table 1. Storage capacity of Roseires Reservoir in million m³ at different years as a function of level, derived from measured bed topographies.

level m above sea level (ID)	origin (1966) volume (Mm³)	1985 volume (Mm³)	1992 volume (Mm³)	2007 volume (Mm³)	2009 volume (Mm³)
465	452	17.13	11.9	9.05	10.88
467	638	60.13	38.97	25.9	26
470	991	259.2	179.8	113	106.6
475	1821	992.8	859	660.5	682.8
480	3024	2082	1937	1701.4	1734.7
481	3329	2337.6	2191.6	1953.8	1984.7

Table 2. The values of physical parameters derived from the calibration process.

Physical parameter	Calibrated value
Spiral flow – (β)	0.5 (-)
Horizontal eddy viscosity	1.0 (m ² /s)
Horizontal eddy diffusivity	10 (m ² /s)
Specific density of sediment	2,650 (kg/m ³)
Csoil (reference density of hindering settling)	1,600 (kg/m ³)
D ₅₀	700 μ m
Dry density of sand	2,000 (kg/m ³)
Dry density of silt (deposited suspended solids)	1,200 (kg/m ³)
W _{s,0} (settling velocity of suspended solids)	0.005 (mm/s)
τ_c (critical shear stress for erosion of silt)	1.0 (N/m ²)
τ_d (critical shear stress for deposition of suspended solids)	1,000 (N/m ²)
M (erosion rate of deposited silt)	2 (mg/m ² /s)

Table 3. Summary of the characteristics of the four trenches.

E*	N*	Trench depth (m)	Location	Nearest village	Distance from main channel (km)**	Distance from dam (km)	Remarks
650539	1280023	2.5	Area 2 (Trench 1)	Ofood	3.4	26	left bank
650537	1280055	4.0	Area 2 (Trench 2)	Ofood	3.4	26	left bank
653332	1284514	4.0	Area 2 (Trench 3)	El Dakhla	1.3	23	right bank
673117	1265608	2.5	Area 1 (Trench 4)	Wad El Mahi	0.4	51	right bank

* These coordinates are in UTM, WGS84, Zone 36North

** When reservoir is empty

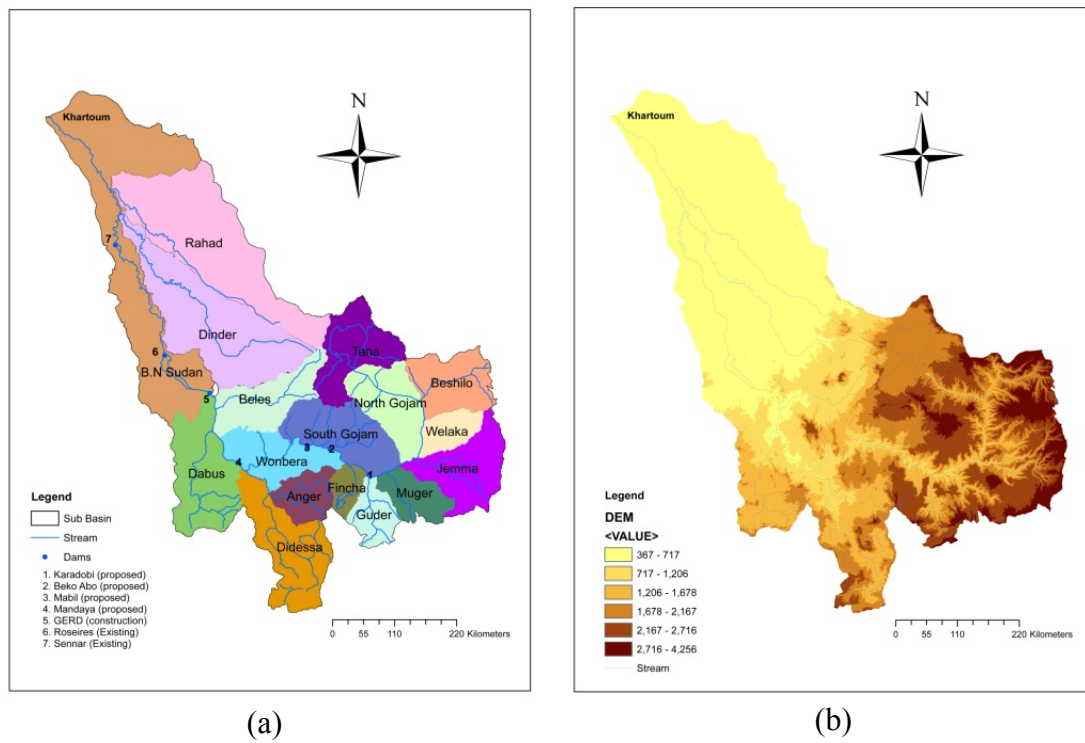


Fig. 1. Blue Nile Basin and Roseires Dam. The elevation map was derived from STRM (90 m) and is in m.a.s.l. (WGS84 Datum).

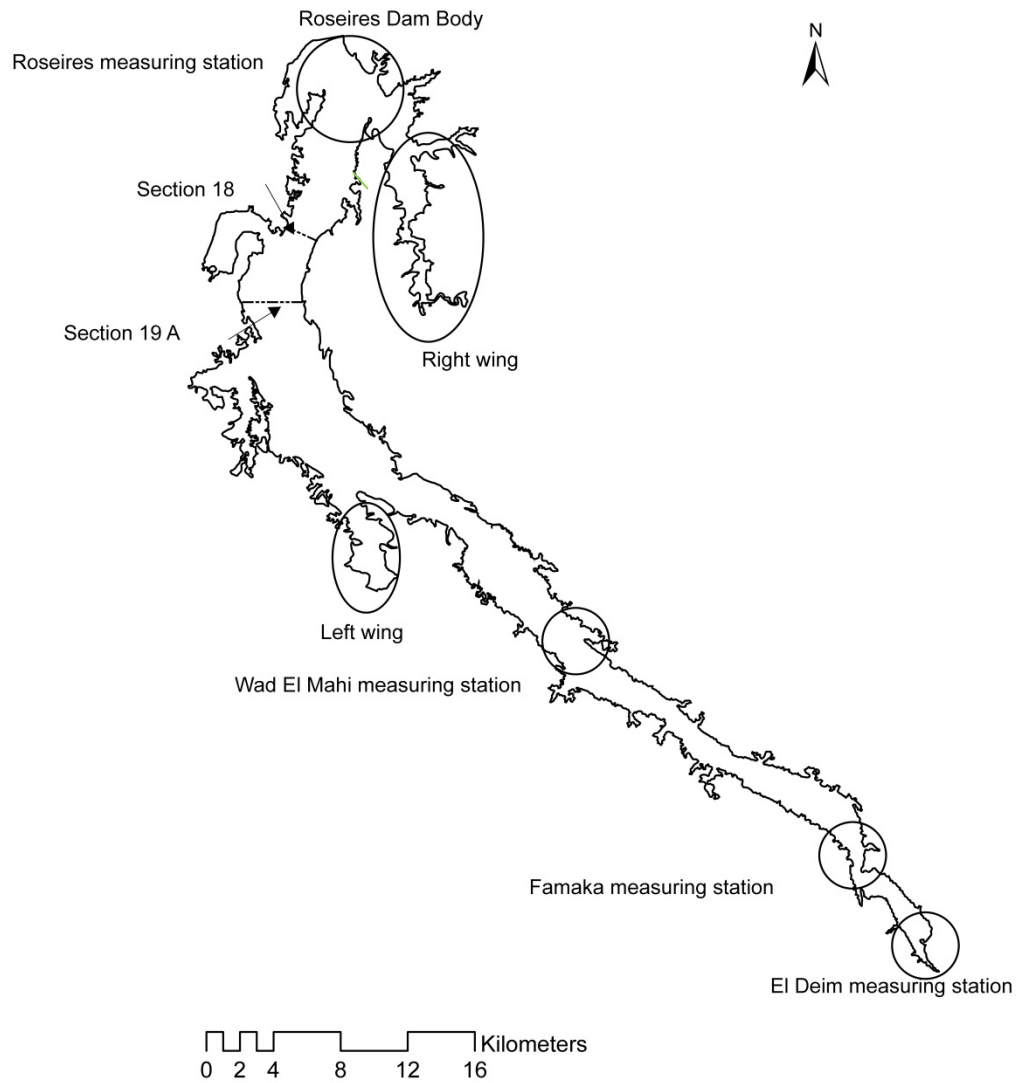


Fig. 2. Measurement stations and the areas (circled) that are not covered by the surveys of 1985 and 1992. The thick black line represents the contour of the reservoir at an elevation of 481 m.a.s.l. (Irrigation Datum).

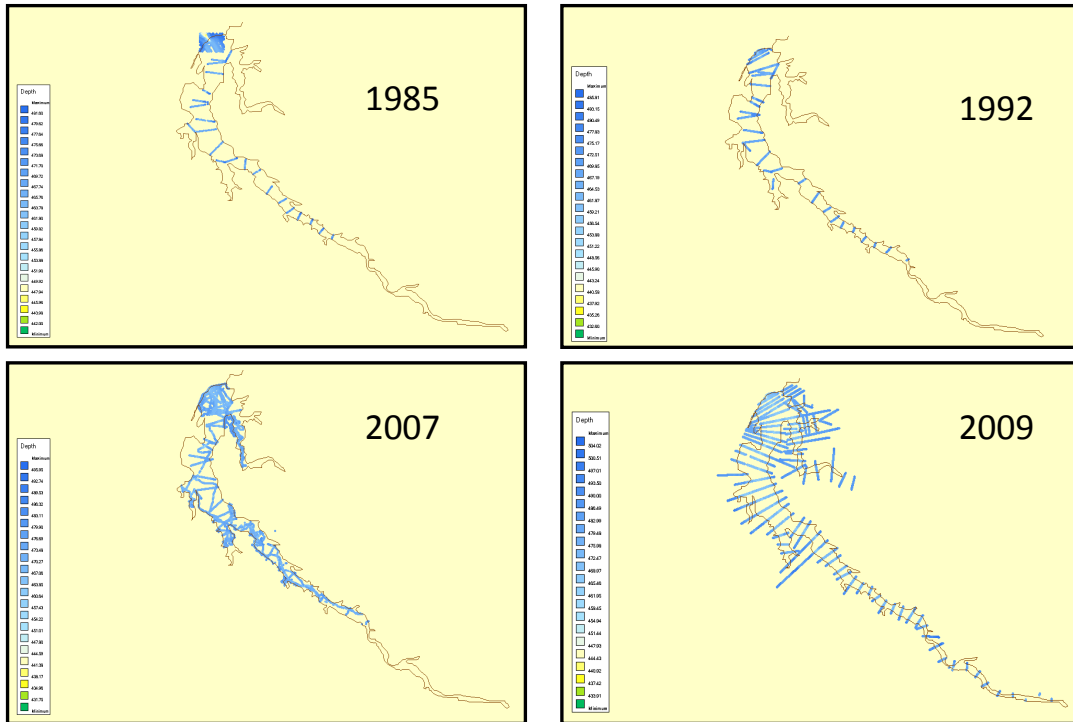


Fig. 3. Available bathymetric surveys (cross-sections).

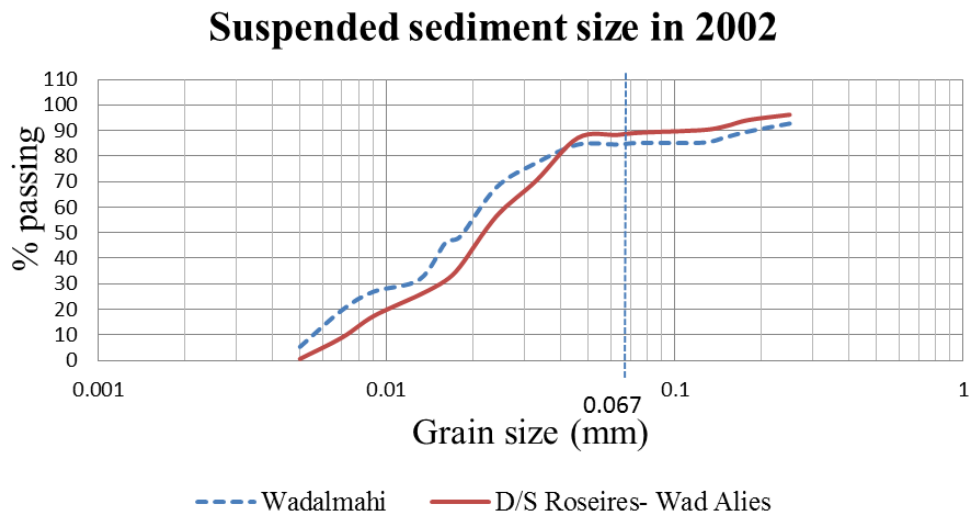


Fig. 4. Suspended sediment grain size distributions inside Roseires Reservoir at Wad El Mahi (location in Fig 2) and downstream of Roseirs Dam (Source: MoIWR).

Surface area of the Roseires Reservoir

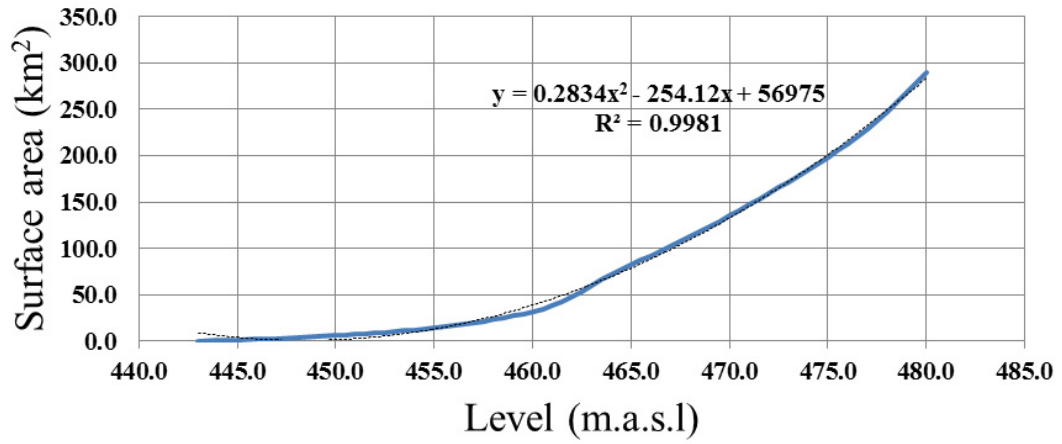


Fig. 5. Water surface area in Roseires Reservoir as a function of elevation (Irrigation Datum). The dotted line represents the trend line used in the study.

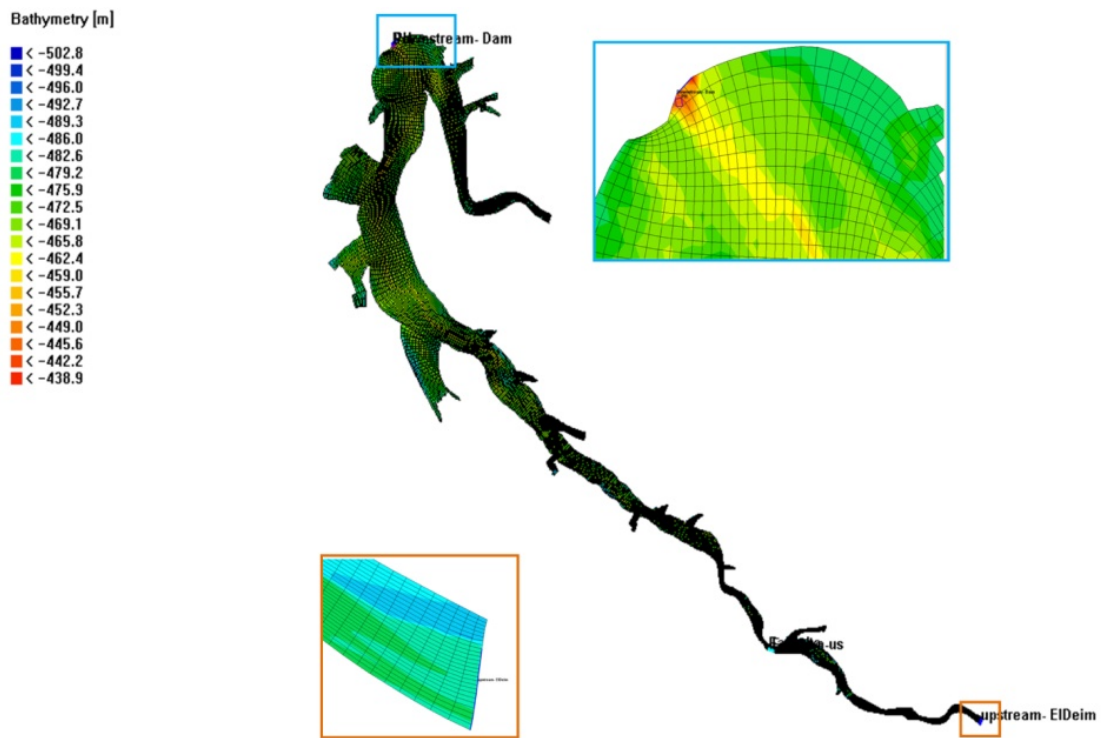


Fig. 6. Upstream and downstream boundaries, computational grid and bed elevations in 2009, in m.a.s.l. (Irrigation Datum).

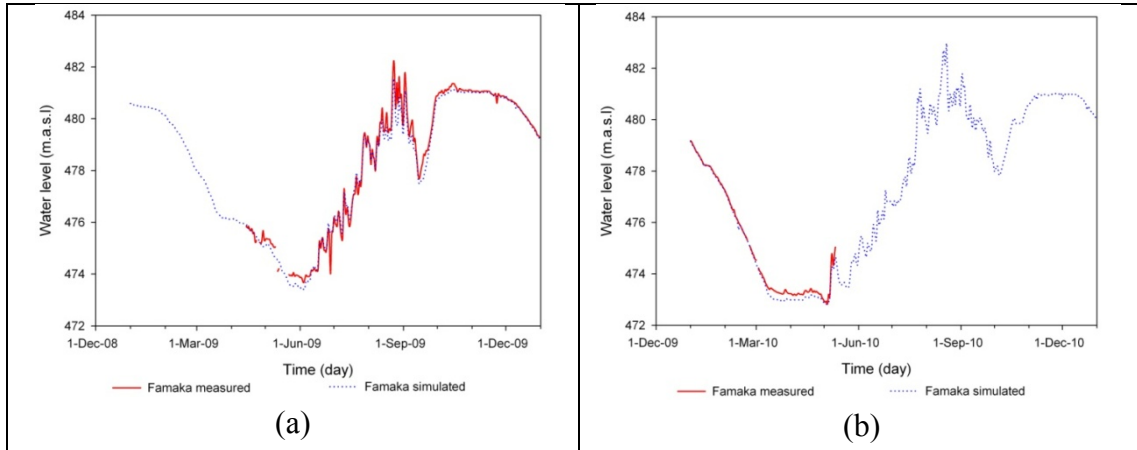


Fig. 7. Results of hydraulic model calibration **(a)** and validation **(b)**: computed vs. measured water levels at Famaka (location in Fig. 2). Levels in m.a.s.l. (Irrigation Datum).

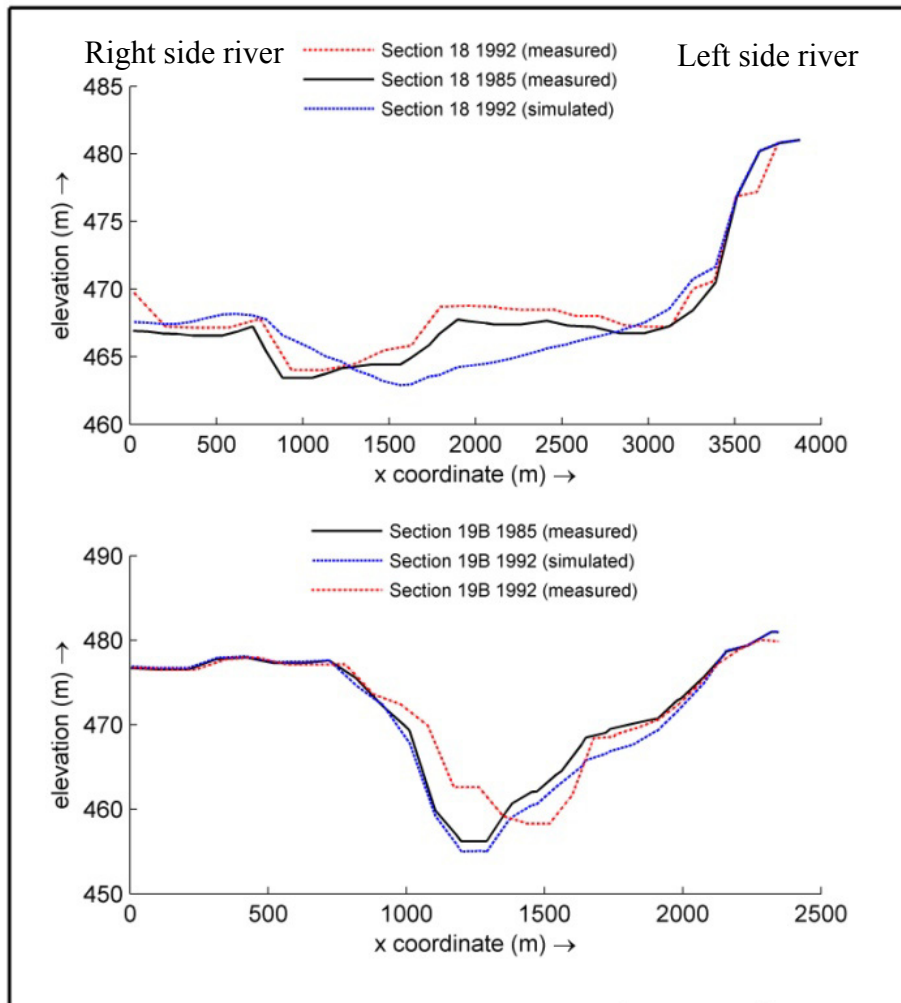


Fig. 8. Cross-sections 18 and 19B seen from downstream. Measured 1985 and 1992 bed elevations and simulated 1992 bed elevation. Cross-section 18 and 19B are located 10.8 km and 15.4 km upstream of the dam, respectively.

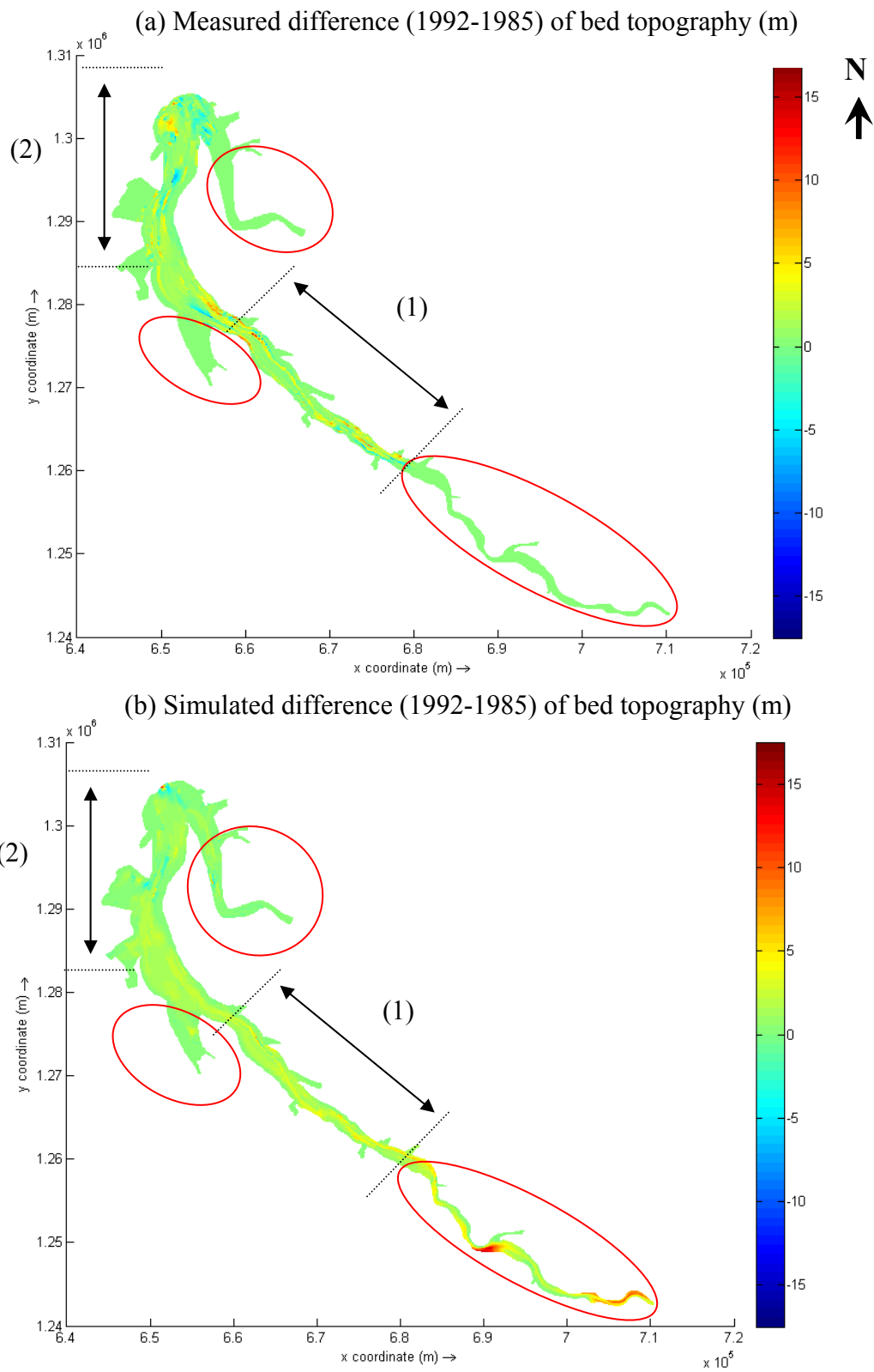


Fig. 9. Comparison between the difference in measured bed topography 1992-1985 and the model cumulative erosion and deposition during the seven-years model run.

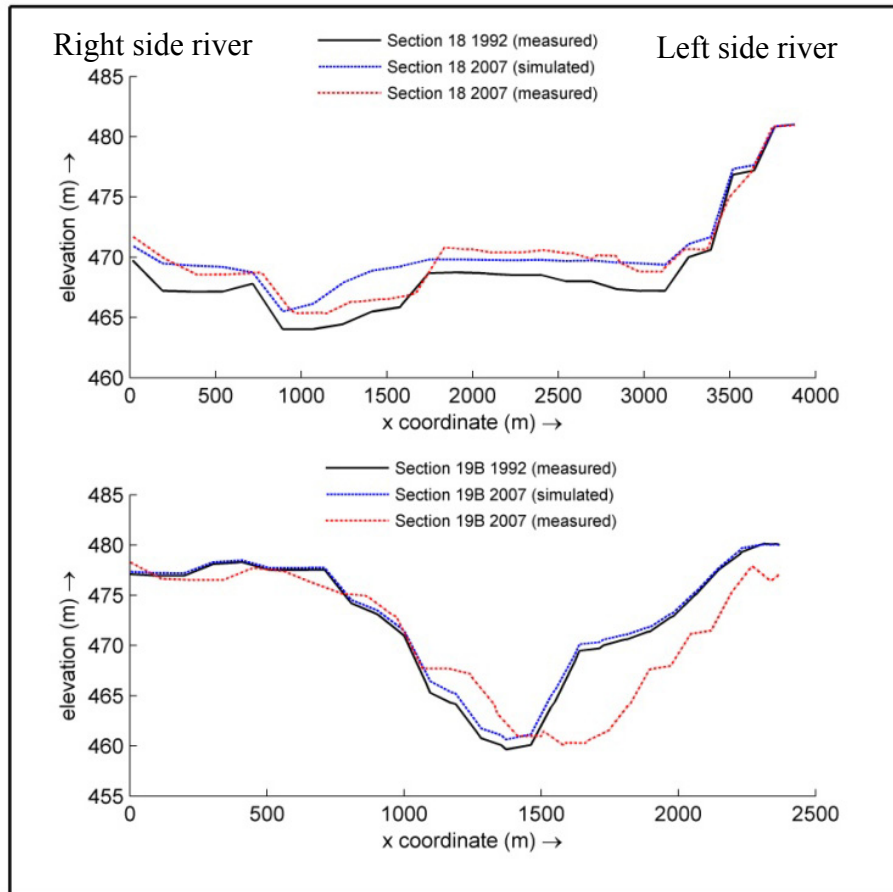


Fig. 10. Cross-sections 18 and 19B seen from downstream. Measured 1992 and 2007 bed elevations and simulated 2007 bed elevation. Cross-section 18 and 19B are located 10.8 km and 15.4 km upstream of the dam, respectively.

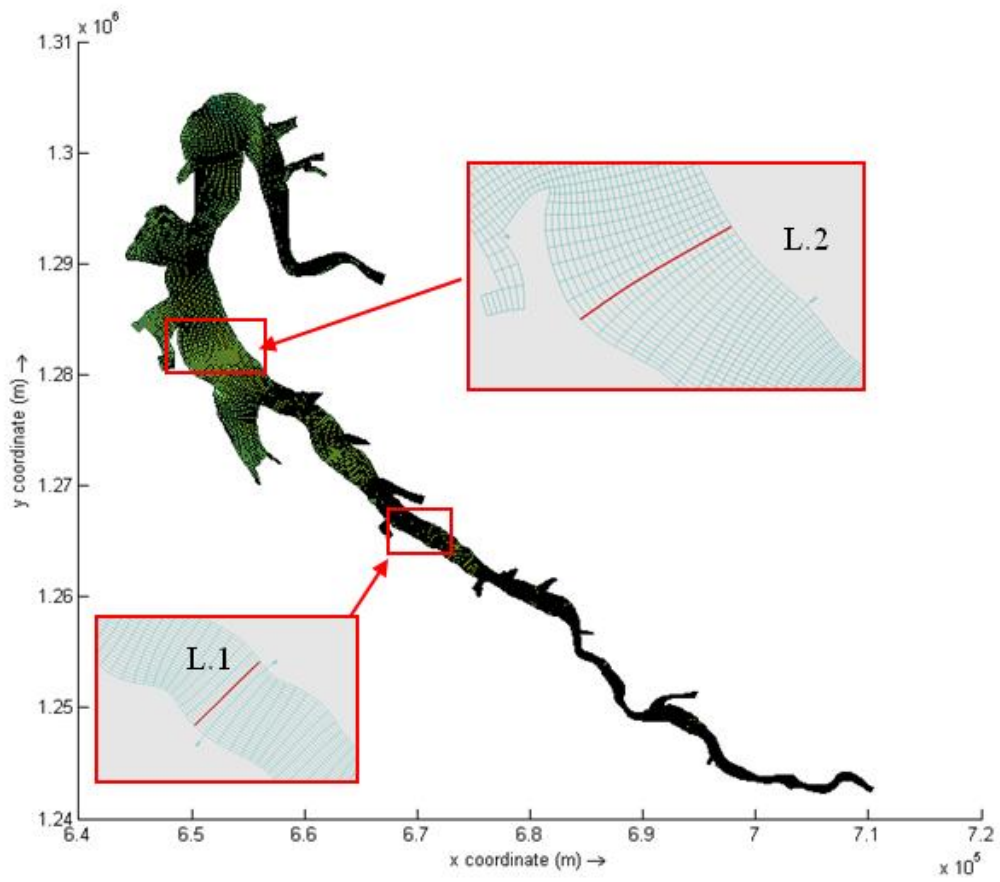


Fig. 11. Selected coring areas (L1 and L2).

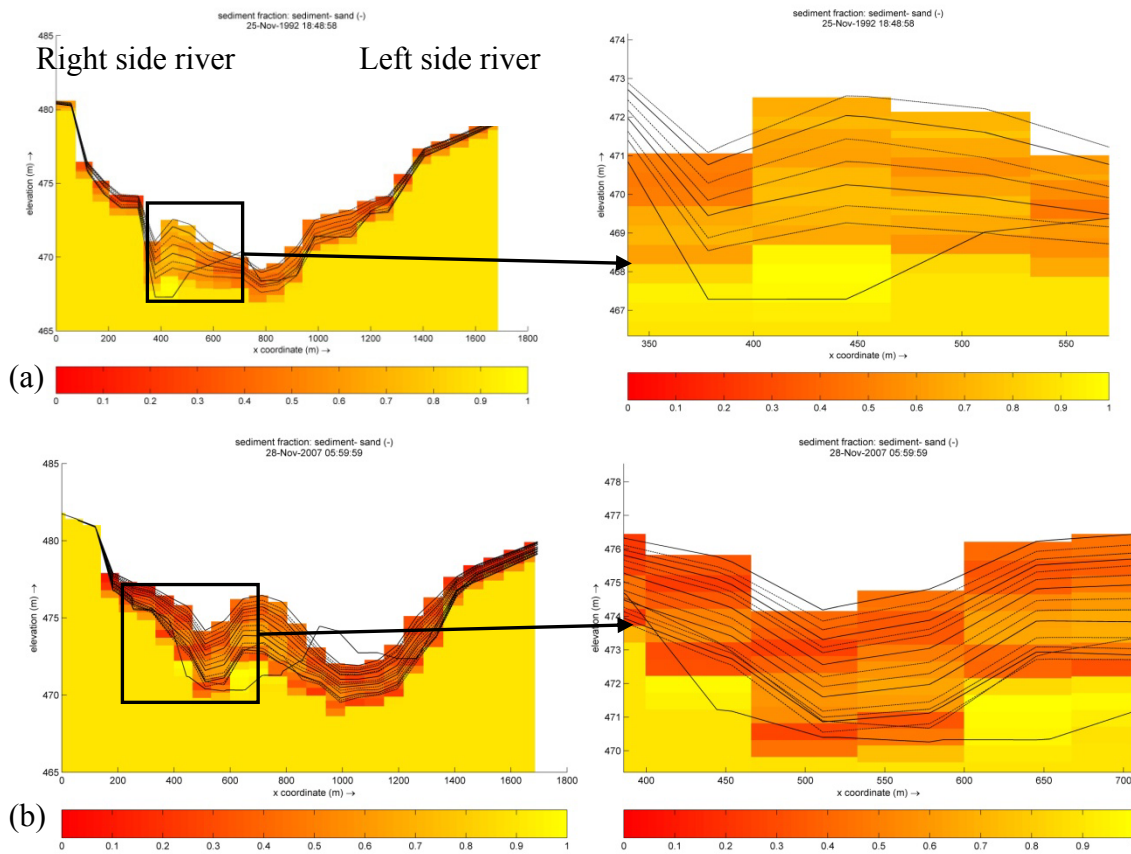


Fig. 12. Vertical profiles of bed composition in Area 1 seen from downstream. Left: entire cross-section. Right: zoomed areas. **(a)** period 1985-1992, **(b)** period 1992-2007. Colour bar: sand content from 0 (red) to 100% (yellow).



Fig. 13. Trench excavation inside Roseires Reservoir.

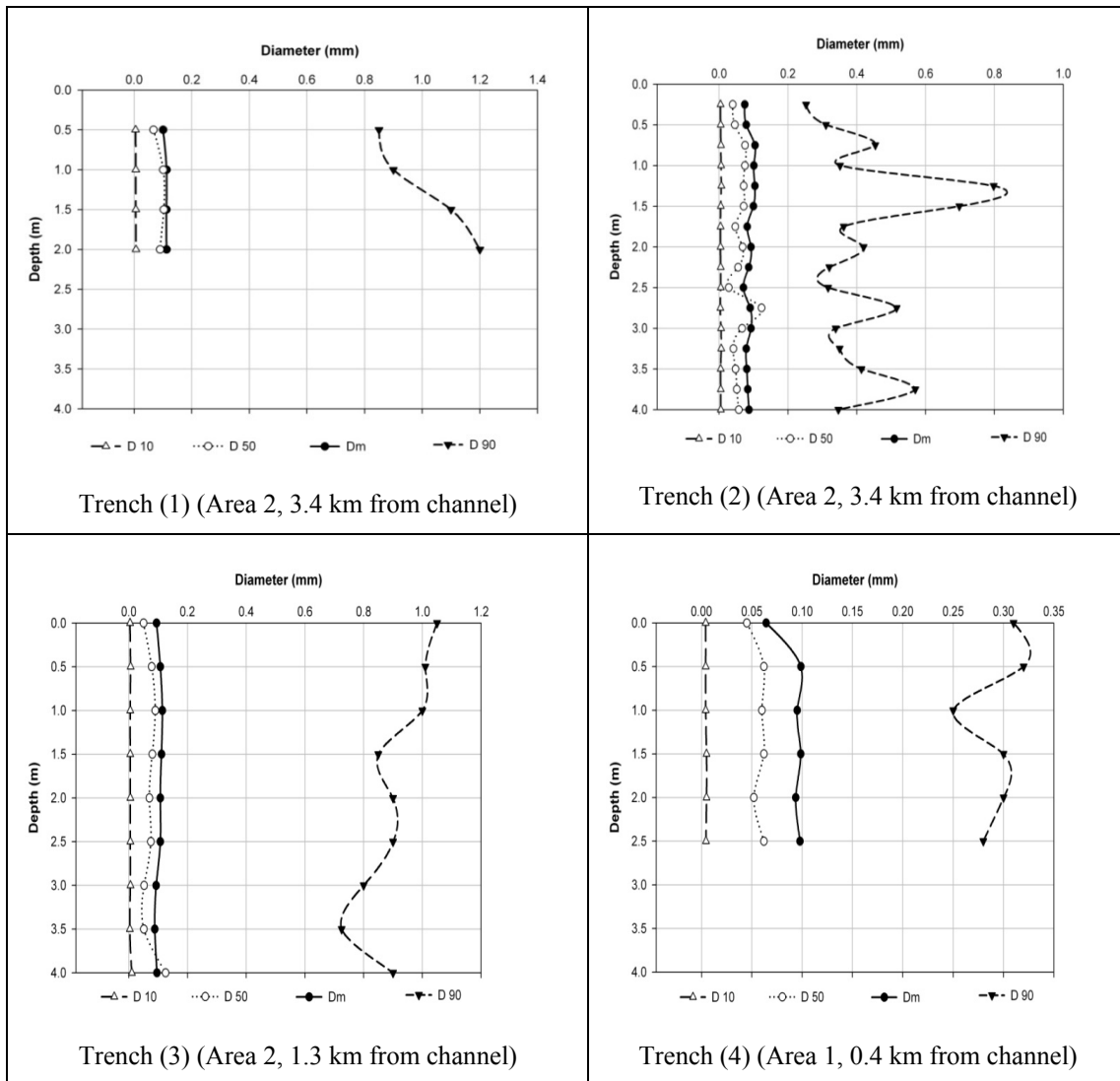


Fig. 14. Soil stratification at the four trenches.